ACS Catalysis

Letter

pubs.acs.org/acscatalysis

# Homogeneous Photochemical Water Oxidation with Cobalt Chloride in Acidic Media

Hongfei Liu,[†] Mauro Schilling,[†] Maxim Yulikov,[‡] Sandra Luber,[†] and Greta R. Patzke*[,†]

[†]Department of Chemistry, University of Zurich, Winterthurerstrasse 190, CH-8057 Zurich, Switzerland

[‡]Laboratory of Physical Chemistry, Department of Chemistry and Applied Biosciences, ETH Zurich, Vladimir-Prelog-Weg 2, CH-8093 Zurich, Switzerland

Supporting Information

**ABSTRACT:** The precise mechanisms of four-electron-transfer water oxidation processes remain to be further understood. Oxide-based precipitation from molecular catalysts as a frequent observation during water oxidation has raised extensive debates on the differentiation between homogeneous and heterogeneous catalysis. Although soluble cobalt salts are known to be active in water oxidation, $CoO_x$ species formed in situ were generally considered to be the true catalyst. Here we report on the possibility homogeneous water oxidation with cobalt chloride in acidic conditions, which prevent $CoO_x$ precipitation. Interestingly, both the buffer media and counteranions were found to significantly influence the oxygen evolution activity, and their roles in the water oxidation process were analyzed with various techniques. This study sheds new light on $Co^{2+}$ ions in key transformation processes of homogeneous water oxidation catalysts.

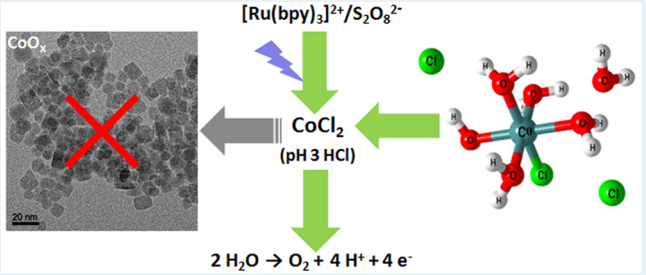


**KEYWORDS:** *homogeneous photochemical water oxidation, cobalt ions, electrochemical water oxidation, buffer influence, counteranion effects*

The current worldwide demand for sustainable solar energy has triggered intense research on solar water splitting.[1] Efficient water oxidation remains a particular challenge in water splitting that calls for the development of robust and economic water oxidation catalysts (WOCs), preferably based on earth-abundant transition metals.[2]

Co-WOCs are in the focus of water oxidation research as a competitive alternative to noble-metal-based catalysts, and a wide range of molecular and (nano)crystalline heterogeneous compounds have been reported over recent years.[3] In 2008, the introduction of self-healing amorphous CoPi catalysts via electrodeposition of $Co^{2+}$ in a pH 7 phosphate buffer[4] aroused widespread interest in amorphous Co, Mn, Fe, and Ni oxides for both electrochemical[5] and photochemical[6] water oxidation. In parallel, forefront investigations at the interface between homo- and heterogeneous WOCs indicated that molecular catalysts frequently act as precatalysts, giving rise to precipitation of oxide species as the true catalysts.[7]

Cobalt ions are a central species in this interplay of water oxidation catalysis types, as outlined by the following inspirational trends: (1) The self-repair mechanisms of CoPi were found to depend on the redeposition of dissolved cobalt ions under electrochemical water oxidation conditions.[8] (2) Several molecular Co-WOCs are in the focus of intense debates concerning their differentiation from active heterogeneous $CoO_x$ catalysts, which may be formed in subsequent processes from leached cobalt ions.[9] (3) Soluble cobalt salts, such as $Co(NO_3)_2$ have long been used as active standards for newly designed WOCs, whose activities they frequently surpass.[7f,9c,10]

This role of cobalt ions as a key player in homo- and heterogeneous catalyst transformations stands in sharp contrast to the actual mechanistic insight into the $Co^{2+}$ pathways of soluble cobalt salts as WOCs. Although some earlier studies proposed $Co^{2+}$ ions as homogeneous catalysts in neutral media,[11] current investigations indicate that $Co^{2+}$ is merely a precatalyst that gives rise to $CoO_x$, $Co(OH)_2$, or CoPi catalysts in situ under photo- or electrochemical conditions.[12] Interestingly, a recent study indicated that $Co^{2+}$ ions may act as homogeneous catalysts during electrochemical water oxidation in acidic conditions.[13]

In the following, we explore the options of homogeneous water oxidation with cobalt chloride in acidic conditions (HCl, pH 3) to avoid precipitations. Moreover, a notable influence of buffer/solution media (citrate, glycine, hydrochloric acid) and counteranions ($Cl^-$, $NO_3^-$, $Br^-$, $ClO_4^-$, and $SO_4^{2-}$) on the water oxidation performance was revealed.

Photochemical water oxidation activity was evaluated according to a standard protocol using $[Ru(bpy)_3]^{2+}$ as the photosensitizer and $S_2O_8^{2-}$ as the electron acceptor. Oxygen evolution was monitored online with Clark electrodes in solution and quantified by gas chromatography (GC) in the

Received: May 26, 2015
Revised: July 20, 2015
Published: July 24, 2015





DOI: 10.1021/acscatal.5b01101
ACS Catal. 2015, 5, 4994−4999

headspace. Control experiments with $CoCl_2$, $Na_2S_2O_8$, photosensitizer, or combinations thereof demonstrate that oxygen evolution requires the presence of all three components (Figure S1), thus confirming the catalytic role of $CoCl_2$. $H_2O$ was verified as oxygen source with $^{18}O$ labeling experiments (Figures S2–S3).

The exact superposition of the $^1H$ NMR spectra of the solution before and after water oxidation (Figure S4) points to a constant concentration of $Co^{2+}$ during water oxidation, that is, the absence of Co-related precipitations, because the peak width varies with the concentration of paramagnetic $Co^{2+}$ ions.[12b] Homogeneous water oxidation is further corroborated by the absence of any peaks arising from insoluble particles in dynamic light-scattering (DLS) measurements (Figure S5). In addition, the solution remained transparent after water oxidation (Figure S6a) without further visual changes, even after a storage period of 5 months (Figure S6b). These observations are in line with the thermodynamic instability[14] of $CoO_x$ under the given conditions. Formation of secondary molecular cobalt related WOCs through complex formation with 2,2′-bipyridine ligands dissociated from $[Ru(bpy)_3]^{2+}$ (cf. reference spectra in Figure S8) was excluded because of negligible oxygen evolution upon addition of 2,2′-bipyridine to the standard reaction protocol (Figure S9).

The influence of $CoCl_2$ concentration on the photochemical water oxidation performance was investigated over a wide concentration range of 0.1–50 mM (Figures 1 and S10). In

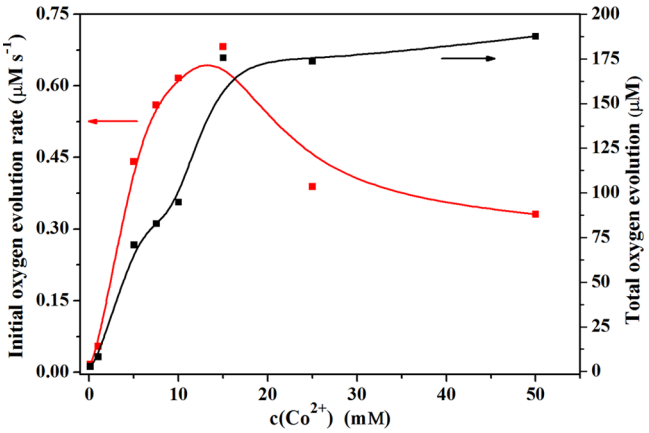


**Figure 1.** Initial oxygen evolution rate during photochemical water oxidation with $CoCl_2$ (10.5 mM $Na_2S_2O_8$, 0.83 mM $[Ru(bpy)_3]Cl_2$; oxygen evolution was online monitored by Clark electrode in solution; visual guidelines have been added).

contrast to previous studies, which revealed high activities for 2 μM $Co^{2+}$ in basic conditions,[9c] no significant activity was observed below 1 mM. This activity difference strongly points to a different water oxidation pathway in basic conditions, implying that heterogeneous $CoO_x$ is the active catalyst. Although the total oxygen evolution amount keeps increasing with the $CoCl_2$ concentration, the initial oxygen evolution rate reaches a maximum at around 15 mM.

Electron paramagnetic resonance (EPR) measurements were conducted to investigate the intermediate species during water oxidation (Figure 2). A mixed solvent ($CH_3CN$ and pH 3 HCl in 2:1 volume ratio) was used to protect the quartz capillary sample holders from freezing damage. Oxygen evolution in this mixed solvent system was confirmed in reference experiments (Figure S12). Background measurements with $[Ru(bpy)_3]^{2+}$/

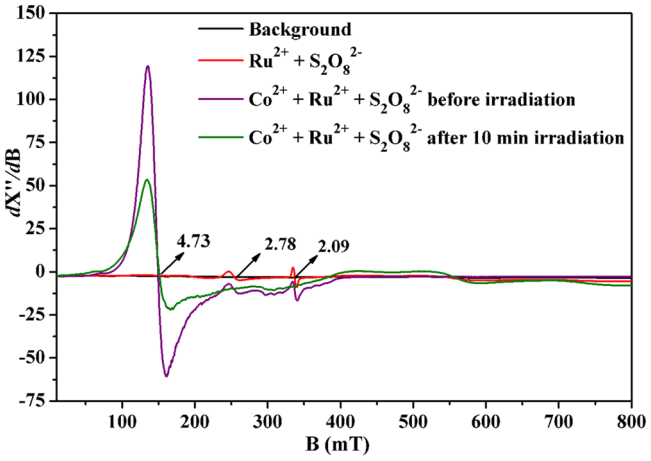


**Figure 2.** EPR spectra (10 K) of $[Ru(bpy)_3]Cl_2$ (10 mM), $Na_2S_2O_8$ (50 mM), and $CoCl_2$(0.83 mM) mixtures (solvent: $CH_3CN$ and pH 3 HCl in 1:2 volume ratio; the solution was frozen after 10 min of irradiation in liquid $N_2$ within less than 5 s).

$Na_2S_2O_8$ mixtures displayed two low-intensity bands of the $[Ru(bpy)_3]^{3+}$ and $SO_4^{\bullet-}$ radicals at $g$ = 2.78 and $g$ = 2.09, respectively. Small amounts of $[Ru(bpy)_3]^{3+}$ are formed from autoxidation of $[Ru(bpy)_3]^{2+}$ in the presence of $Na_2S_2O_8$ and natural light. Addition of $CoCl_2$ gave rise to a strong absorption band of paramagnetic $Co^{2+}$, with the most intense peak at $g$ = 4.73 and a shoulder extended to $g \sim 2.00$. Similar spectra were reported for $Co(NO_3)_2$, which can be assigned to high spin $Co^{2+}$.[5d] However, a notable intensity decrease by ∼50% was observed after 10 min of irradiation at 460 nm, most probably due to the partial oxidation of $Co^{2+}$ to EPR-silent $Co^{3+}$ species. This was accompanied by the disappearance of the $[Ru(bpy)_3]^{3+}$ and $SO_4^{\bullet-}$ radical bands in the course of the water oxidation. In contrast to recent reports on molecular Co-WOCs,[15] the suggested $Co^{4+}$ intermediate species with a characteristic resonance at $g \sim 2.00$[5d] was not observed under the present conditions, probably implying a different water oxidation pathway in acidic conditions. Spontaneous release of oxygen observed for specific $Co^{3+}$ complexes, such as $[Co(H_2O)_6]^{3+}$, furthermore indicates that $Co^{4+}$ species are not indispensable for oxygen evolution, especially in acidic media.[16]

Furthermore, the influence of different buffer media on the water oxidation activity of $CoCl_2$ at pH 3 was investigated in detail. The general advantages of buffers in water oxidation systems include the prevention of a sharp pH decrease and the facilitation of proton-coupled electron transfer processes.[17] However, the highest oxygen evolution with $CoCl_2$ WOCs was observed in nonbuffered HCl solution, and glycine and potassium citrate buffers had a detrimental effect on the overall activity (Figure 3). This trend indicates that buffer ions significantly influence the water oxidation performance. Further information on their coordination to $Co^{2+}$ centers was obtained by density functional theory calculations. Coordination of citrate (Figures S34–S36) and glycine (Figure S37) buffer molecules to $[Co(H_2O)_6]^{2+}$ complexes was investigated in more detail and allowed to identify a range of possible isomers as well as energetically preferred coordination modes. The computed reaction free energies also support a strong binding of the tridentate citrate molecule to the $Co^{2+}$ ion.

UV/vis and $^1H$ NMR spectroscopic characterizations of $Co^{2+}$ species in different buffer media point in the same direction


DOI: 10.1021/acscatal.5b01101
ACS Catal. 2015, 5, 4994–4999

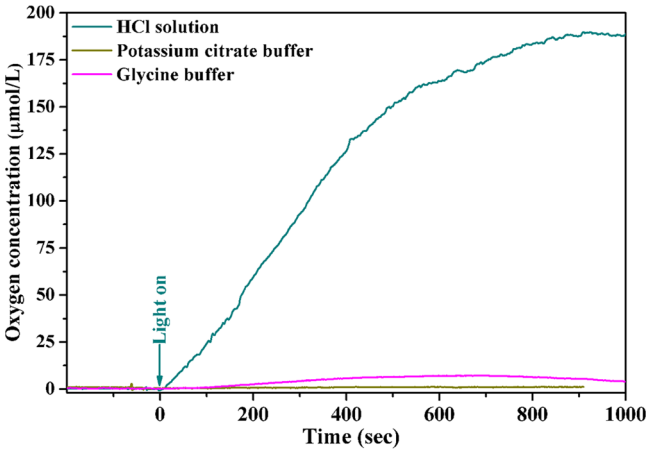


**Figure 3.** Photochemical water oxidation with $CoCl_2$ in buffered vs nonbuffered conditions (52.6 mM $CoCl_2$, 10.5 mM $Na_2S_2O_8$, 0.83 mM $[Ru(bpy)_3]Cl_2$, 0.1 M pH 3 buffer medium or pH 3 HCl).

(Figure 4). The absorption intensity of $Co^{2+}$ at 450−550 nm decreased in the following order: potassium citrate buffer > glycine buffer > HCl solution (Figure S17, the absorption difference related to HCl solution is shown in Figure 4d). This is in line with the water oxidation activity trends: peak performance at pH 3 (HCl), followed by a weak but detectable oxygen evolution in glycine buffer and inactivity in potassium citrate buffer. Comparison of the respective $^1H$ signals around 4.7 ppm and of the buffer-related peaks in the $^1H$ NMR spectra illustrates these different complexing properties in a more straightforward manner (Figures 4a−c). The presence of paramagnetic $Co^{2+}$ leads to a line-broadening and shift to 4.82 ppm for HCl and glycine media, whereas the stronger coordination of citrate anions to the cobalt centers increases the peak shift to 4.85 ppm. Concerning the buffer peaks, the characteristic signal of glycine at 3.55 ppm is shifted to 2.97 ppm, with a notably lower intensity that indicates weaker and nonquantitative coordination to $Co^{2+}$ (Figure 4b). Accordingly, the water oxidation activity is slightly improved in dilute glycine media (Figure S18). The stronger and more efficient complexation of the $Co^{2+}$ centers by the citrate buffer is evident from the disappearance of the four peaks corresponding to citrate (2.73, 2.78, 2.88, and 2.93 ppm; Figure 4c). These results highlight that buffer media can indeed exert an adverse effect on the oxygen evolution performance.

Electron transfer processes as another crucial parameter for water oxidation efficiency were investigated by laser flash photolysis. Generally, deactivation of the excited $[Ru(bpy)_3]^{2+*}$ photosensitizer follows two main pathways, namely, either relaxation to $[Ru(bpy)_3]^{2+}$ via fluorescence or persulfate quenching to $[Ru(bpy)_3]^{3+}$ and subsequent regeneration to $[Ru(bpy)_3]^{2+}$ by hole transfer to the WOC. Because the fluorescence lifetime of $[Ru(bpy)_3]^{2+*}$ is in the 200−300 ns range (Figure S19), the absorption bleaching of $[Ru(bpy)_3]^{2+}$ after irradiation on the microsecond scale arises from the formation of $[Ru(bpy)_3]^{3+}$. The faster the recovery of the $[Ru(bpy)_3]^{2+}$ absorption, the more efficient the hole injection from $[Ru(bpy)_3]^{3+}$ to WOC. Flash photolysis measurements in citrate buffer display a strong absorption bleaching after irradiation at around 40 $\mu$s, followed by immediate recovery to a certain level through fluorescence within 279 ns (Figure S19). The absorption level remains constantly low without further increase up to 100 $\mu$s (Figure 5), thus indicating the absence of hole transfer between $[Ru(bpy)_3]^{3+}$ and WOCs. This agrees well with the observed water oxidation inactivity of $CoCl_2$ in potassium citrate buffer. In contrast, the absorption bleaching of $[Ru(bpy)_3]^{2+}$ in both glycine buffer and HCl solution displays gradual recovery (Figure 5). The notably higher oxygen evolution observed in HCl solution exactly agrees with the faster absorption recovery within no more than 60 $\mu$s compared with glycine buffer. The analogous trends of UV/vis, $^1H$ NMR, and hole injection rate for different solutions/buffers strongly suggest a significant influence of the coordinative effects of the buffer/solution compositions on the catalytic performance.

The electrochemical water oxidation activity of $Co^{2+}$ centers in buffered (pH 3) and nonbuffered conditions was furthermore compared with the photochemical results. The

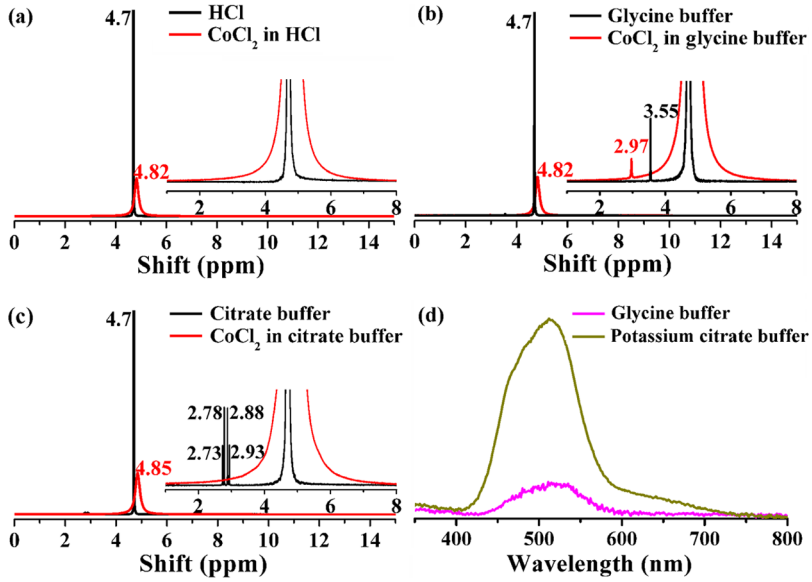


**Figure 4.** $^1H$ NMR (a−c) and UV/vis absorption (d) spectra in buffered or nonbuffered conditions. (168.1 mM $CoCl_2$, 0.01 M buffer, solvent: $H_2O/D_2O$ = 1/9).



DOI: 10.1021/acscatal.5b01101
ACS Catal. 2015, 5, 4994−4999

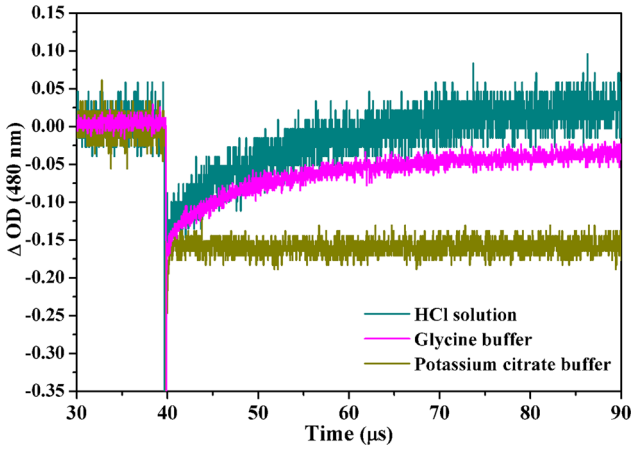


**Figure 5.** Transient absorption of $[Ru(bpy)_3]^{2+}$ at 480 nm after irradiation with a 355 nm laser (10.5 M $CoCl_2$, 2.1 mM $Na_2S_2O_8$, 0.17 mM $[Ru(bpy)_3]Cl_2$; absorption intensities were normalized for comparison).

detrimental influence of buffer media on water oxidation is also evident from the electrochemical results (Figure 6). Reference

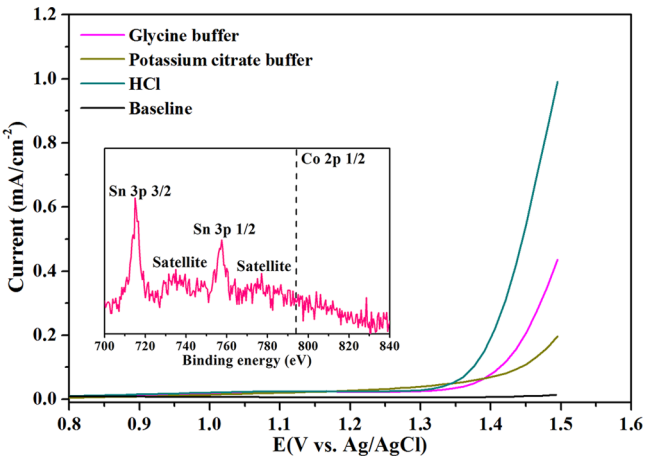


**Figure 6.** Electrochemical water oxidation in buffered vs nonbuffered conditions (63.0 mM $CoCl_2$, 0.1 M buffer, pH 3; inset: absence of Co in XPS spectra of the FTO electrode after electrochemical water oxdiation).

experiments with an additional electrolyte (Figure S33) showed that conductivity differences of the electrolyte solutions did not exert a significant effect on the electrocatalytic performance (Figure S33). Thus, the electrochemical performance difference in different buffer media is not arising from their conductivity difference.

The strongly buffer-dependent performance indicates that the role of the buffer includes far more effects than just stabilizing the pH level or facilitating PCET. Adverse buffer effects, such as slower electron transfer rates and, most importantly, blocking of active catalyst sites, may even outweigh their benefits.[18] This was recently demonstrated for the notable influence of the electrolyte on heterogeneous electrocatalysts, such as the CoPi OEC.[5a,13] The self-healing mechanisms of these WOCs probably imply a partial contribution of homogeneous water oxidation processes mediated by the release of $Co^{2+}$ cations into solution.

The deposition of secondary heterogeneous Co-electrocatalysts on the electrode surface was excluded with several analytical methods. First, EDS spectra of the FTO electrodes after water oxidation (Figure S20) did not display any cobalt signals. Moreover, electrodes were rinsed with water after $CoCl_2$-assisted water oxidation and tested for water oxidation in freshly prepared HCl (pH 3) solution in the absence of $CoCl_2$. The rinsed FTO electrodes did not display different currents compared with blank reference FTO electrodes (Figure S21), indicating that no WOC active species were deposited on the surface. Moreover, ICP-AES analyses of the Co contents of FTO electrode samples before and after 50 water oxidation cycles afforded values below the detection limit of 0.1 $\mu$mol throughout. XPS as a more sensitive technique was used to screen the FTO electrodes for residual cobalt after water oxidation. As shown in the inset of Figure 6, the characteristic Co $2p_{1/2}$ could not be detected, thus indicating the absence of any cobalt precipitation.

In addition to the exploration of the effect of different buffer media, the influence of the counteranion on the water oxidation performance was investigated for $Co(NO_3)_2$ in $HNO_3$ (pH 3) with respect to photo- and electrochemical water oxidation. The presence of $NO_3^-$ turned out to be detrimental for the photochemical performance in the presence of $Co^{2+}$ cations (Figure S23). The same trend was observed in electrochemical investigations (Figure S24). Further reference experiments with $CoBr_2$, $Co(ClO_4)_2$, and $CoSO_4$ for photochemical water oxidation indicate that the activity of $CoBr_2$ is comparable to $CoCl_2$, whereas $Co(ClO_4)_2$ displays minor activity, and $CoSO_4$ is completely inactive (Figure S25; note that $CoBr_2$ forms a precipitate). These remarkably different activity trends highlight the complex behavior toward parameter changes of this simple oxygen evolving system based on cobalt salts.

Reference experiments with $NiCl_2$, $MnCl_2$, and $FeCl_3$ were investigated for water oxidation, as well (Figures S26–S31). All of these systems displayed considerably lower water oxidation activities under comparable conditions. $MnCl_2$ was entirely inactive and formed amorphous manganese oxide precipitates during photochemical (photographs: Figure S27, PXRD pattern: Figure S28) and electrochemical (photographs: Figure S32) water oxidation, but $NiCl_2$ and $FeCl_3$ solutions remained homogeneous.

The respective influence of the counteranions ($Cl^-$, $NO_3^-$, $Br^-$, $ClO_4^-$, and $SO_4^{2-}$) and cations ($Co^{2+}$, $Ni^{2+}$, $Fe^{2+}$, and $Mn^{2+}$) on the water oxidation activity remains to be clarified with detailed studies. Concerning $CoCl_2$ in pH 3 HCl, $[Co[(H_2O)_5Cl]^+$ is one of the major $Co^{2+}$ species.[19] Chloride coordination is thus likely to exert a certain influence on the water oxidation process. A recent study furthermore indicated that $Cl^-$ can be more easily oxidized to chlorine after complexation into $[AgCl_2]^-$ in the presence of $Ag^+$.[20] We explored this possibility for $Co^{2+}$, as well, in the present study by GC/MS measurements; however, no chlorine was detected under the present conditions. A follow-up mechanistic study to differentiate the respective influence of transition metal cations and their counteranions on the water oxidation is underway.

In summary, we have newly investigated simple cobalt salts for water oxidation in a selected parameter window (pH 3) that prevents the formation of $CoO_x$. However, this exploration of homogeneous water oxidation with cobalt salts under acidic conditions came at the cost of rather moderate activity. It is noteworthy that the presence of different buffer systems dramatically reduced both photo- and electrochemical oxygen



DOI: 10.1021/acscatal.5b01101
ACS Catal. 2015, 5, 4994–4999

evolution. This sheds new light on the crucial role of the buffer media in water oxidation, which goes beyond mere proton reservoirs. The significant role of counteranions in the water oxidation process was revealed, as well. Further investigations on the influence of counteranions on the underlying water oxidation reaction pathways are now in progress.

## ■ ASSOCIATED CONTENT

### Supporting Information

The Supporting Information is available free of charge on the ACS Publications website at DOI: 10.1021/acscatal.5b01101.

Experimental details and further data (additional photochemical and electrochemical water oxidation results, $^{1}$H NMR, DLS, SEM-EDX, and UV/vis data, $^{18}$O labeling experiments, and quantum chemical calculations) (PDF)

## ■ AUTHOR INFORMATION


### Corresponding Author

*E-mail: greta.patzke@chem.uzh.ch.


### Notes

The authors declare no competing financial interests.

## ■ ACKNOWLEDGMENTS

Financial support by the Swiss National Science Foundation (Sinergia Grant No. CRSII2_136205/1) is gratefully acknowledged. The work has been supported by the University Research Priority Program (URPP) for solar light to chemical energy conversion (LightChEC). We thank Dr. Jörg Patscheider (EMPA Dübendorf) for XPS measurements and Johannes Windisch, Dr. Benjamin Probst-Rüd, and Prof. Roger Alberto (Department of Chemistry, UZH) for experimental support and helpful discussions. H.L. thanks the China Scholarship Council for a PhD fellowship.

## ■ REFERENCES


(1) (a) Dismukes, G. C.; Brimblecombe, R.; Felton, G. A. N.; Pryadun, R. S.; Sheats, J. E.; Spiccia, L.; Swiegers, G. F. *Acc. Chem. Res.* **2009**, *42*, 1935−1943. (b) Berardi, S.; Drouet, S.; Francàs, L.; Gimbert-Suriach, C.; Guttentag, M.; Richmond, C.; Stoll, T.; Llobet, A. *Chem. Soc. Rev.* **2014**, *43*, 7501−7519. (c) Swierk, J. R.; Mallouk, T. E. *Chem. Soc. Rev.* **2013**, *42*, 2357−2387. (d) Alibabaei, L.; Brennaman, M. K.; Norris, M. R.; Kalanyan, B.; Song, W.; Losego, M. D.; Concepcion, J. J.; Binstead, R. A.; Parsons, G. N.; Meyer, T. J. *Proc. Natl. Acad. Sci. U. S. A.* **2013**, *110*, 20008−20013. (e) Antonietti, M. *Angew. Chem., Int. Ed.* **2013**, *52*, 1086−1087.

(2) (a) Sartorel, A.; Bonchio, M.; Campagna, S.; Scandola, F. *Chem. Soc. Rev.* **2013**, *42*, 2262−2280. (b) McAlpin, J. G.; Stich, T. A.; Casey, W. H.; Britt, R. D. *Coord. Chem. Rev.* **2012**, *256*, 2445−2452. (c) Singh, A.; Spiccia, L. *Coord. Chem. Rev.* **2013**, *257*, 2607−2622. (d) Crabtree, R. H. *Chem. Rev.* **2012**, *112*, 1536−1554. (e) Jiao, F.; Frei, H. *Energy Environ. Sci.* **2010**, *3*, 1018−1027. (f) Young, K. J.; Martini, L. A.; Milot, R. L.; Snoeberger, R. C., III; Batista, V. S.; Schmuttenmaer, C. A.; Crabtree, R. H.; Brudvig, G. W. *Coord. Chem. Rev.* **2012**, *256*, 2503−2520. (g) Takashima, T.; Hashimoto, K.; Nakamura, R. *J. Am. Chem. Soc.* **2012**, *134*, 1519−1527. (h) Santoni, M.-P.; La Ganga, G.; Mollica Nardo, V.; Natali, M.; Puntoriero, F.; Scandola, F.; Campagna, S. *J. Am. Chem. Soc.* **2014**, *136*, 8189−8192. (i) Bloor, L. G.; Molina, P. I.; Symes, M. D.; Cronin, L. *J. Am. Chem. Soc.* **2014**, *136*, 3304−3311. (j) Pintado, S.; Goberna-Ferrón, S.; Escudero-Adán, E. C.; Galán-Mascarós, J. R. *J. Am. Chem. Soc.* **2013**, *135*, 13270−13273.

(3) (a) Del Pilar-Albaladejo, J.; Dutta, P. K. *ACS Catal.* **2014**, *4*, 9−15. (b) Ahn, H. S.; Yano, J.; Tilley, T. D. *ACS Catal.* **2015**, *5*, 2573−2576. (c) Liu, H.; Patzke, G. R. *Chem. - Asian J.* **2014**, *9*, 2249−2259. (d) Wasylenko, D. J.; Palmer, R. D.; Berlinguette, C. P. *Chem. Commun.* **2013**, *49*, 218−227. (e) Chen, M.; Ng, S.-M.; Yiu, S.-M.; Lau, K.-C.; Zeng, R. J.; Lau, T.-C. *Chem. Commun.* **2014**, *50*, 14956−14959. (f) Smith, P. F.; Kaplan, C.; Sheats, J. E.; Robinson, D. M.; McCool, N. S.; Mezle, N.; Dismukes, G. C. *Inorg. Chem.* **2014**, *53*, 2113−2121. (g) Yin, Q.; Tan, J. M.; Besson, C.; Geletii, Y. V.; Musaev, D. G.; Kuznetsov, A. E.; Luo, Z.; Hardcastle, K. I.; Hill, C. L. *Science* **2010**, *328*, 342−345. (h) Goberna-Ferrón, S.; Hernandez, W. Y.; Rodriguez-Garcia, B.; Galán-Mascarós, J. R. *ACS Catal.* **2014**, *4*, 1637−1641.

(4) Kanan, M. W.; Nocera, D. G. *Science* **2008**, *321*, 1072−1075.

(5) (a) Surendranath, Y.; Dincă, M.; Nocera, D. G. *J. Am. Chem. Soc.* **2009**, *131*, 2615−2620. (b) Bediako, D. K.; Lassalle-Kaiser, B.; Surendranath, Y.; Yano, J.; Yachandra, V. K.; Nocera, D. G. *J. Am. Chem. Soc.* **2012**, *134*, 6801−6809. (c) Risch, M.; Khare, V.; Zaharieva, I.; Gerencser, L.; Chernev, P.; Dau, H. *J. Am. Chem. Soc.* **2009**, *131*, 6936−6937. (d) McAlpin, J. G.; Surendranath, Y.; Dincă, M.; Stich, T. A.; Stoian, S. A.; Casey, W. H.; Nocera, D. G.; Britt, R. D. *J. Am. Chem. Soc.* **2010**, *132*, 6882−6883. (e) Hu, S.; Shaner, M. R.; Beardslee, J. A.; Lichterman, M.; Brunschwig, B. S.; Lewis, N. S. *Science* **2014**, *344*, 1005−1009. (f) Smith, R. D. L.; Prévot, M. S.; Fagan, R. D.; Zhang, Z.; Sedach, P. A.; Siu, M. K. J.; Trudel, S.; Berlinguette, C. P. *Science* **2013**, *340*, 60−63. (g) Kanan, M. W.; Yano, J.; Surendranath, Y.; Dincă, M.; Yachandra, V. K.; Nocera, D. G. *J. Am. Chem. Soc.* **2010**, *132*, 13692−13701. (h) Indra, A.; Menezes, P. W.; Zaharieva, I.; Baktash, E.; Pfrommer, J.; Schwarze, M.; Dau, H.; Driess, M. *Angew. Chem., Int. Ed.* **2013**, *52*, 13206−13210. (i) Kuai, L.; Geng, J.; Chen, C.; Kan, E.; Liu, Y.; Wang, Q.; Geng, B. *Angew. Chem., Int. Ed.* **2014**, *53*, 7547.

(6) (a) Indra, A.; Menezes, P. W.; Zaharieva, I.; Baktash, E.; Pfrommer, J.; Schwarze, M.; Dau, H.; Driess, M. *Angew. Chem., Int. Ed.* **2013**, *52*, 13206−13210. (b) Iyer, A.; Del-Pilar, J.; King'ondu, C. K.; Kissel, E.; Garces, H. F.; Huang, H.; El-Sawy, A. M.; Dutta, P. K.; Suib, S. L. *J. Phys. Chem. C* **2012**, *116*, 6474−6483. (c) Indra, A.; Menezes, P. W.; Sahraie, N. R.; Bergmann, A.; Das, C.; Tallarida, M.; Schmeiβer, D.; Strasser, P.; Driess, M. *J. Am. Chem. Soc.* **2014**, *136*, 17530−17536.

(7) (a) Najafpour, M. M.; Moghaddam, A. N.; Dau, H.; Zaharieva, I. *J. Am. Chem. Soc.* **2014**, *136*, 7245−7248. (b) Hocking, R. K.; Brimblecombe, R.; Chang, L.-Y.; Singh, A.; Cheah, M. H.; Glover, C.; Casey, W. H.; Spiccia, L. *Nat. Chem.* **2011**, *3*, 461−466. (c) Schley, N. D.; Blakemore, J. D.; Subbaiyan, N. K.; Incarvito, C. D.; D'Souza, F.; Crabtree, R. H.; Brudvig, G. W. *J. Am. Chem. Soc.* **2011**, *133*, 10473−10481. (d) Chen, G.; Chen, L.; Ng, S.-M.; Man, W.-L.; Lau, T.-C. *Angew. Chem., Int. Ed.* **2013**, *52*, 1789−1791. (e) Fu, S.; Liu, Y.; Ding, Y.; Du, X.; Song, F.; Xiang, R.; Ma, B. *Chem. Commun.* **2014**, *50*, 2167−2169. (f) Hong, D.; Jung, J.; Park, J.; Yamada, Y.; Suenobu, T.; Lee, Y.-M.; Nam, W.; Fukuzumi, S. *Energy Environ. Sci.* **2012**, *5*, 7606−7616. (g) Chen, G.; Chen, L.; Ng, S.-M.; Lau, T.-C. *ChemSusChem* **2014**, *7*, 127−134. (h) Grotjahn, D. B.; Brown, D. B.; Martin, J. K.; Marelius, D. C.; Abadjian, M.-C.; Tran, H. N.; Kalyuzhny, G.; Vecchio, K. S.; Specht, Z. G.; Cortes-Llamas, S. A.; Miranda-Soto, V.; Van Niekerk, C.; Moore, C. E.; Rheingold, A. L. *J. Am. Chem. Soc.* **2011**, *133*, 19024−19027.

(8) (a) Lutterman, D. A.; Surendranath, Y.; Nocera, D. G. *J. Am. Chem. Soc.* **2009**, *131*, 3838−3839. (b) Surendranath, Y.; Kanan, M. W.; Nocera, D. G. *J. Am. Chem. Soc.* **2010**, *132*, 16501−16509.

(9) (a) Stracke, J. J.; Finke, R. G. *J. Am. Chem. Soc.* **2011**, *133*, 14872−14875. (b) Natali, M.; Berardi, S.; Sartorel, A.; Bonchio, M.; Campagna, S.; Scandola, F. *Chem. Commun.* **2012**, *48*, 8808−8810. (c) Vickers, J. W.; Lv, H.; Sumliner, J. M.; Zhu, G.; Luo, Z.; Musaev, D. G.; Geletii, Y. V.; Hill, C. L. *J. Am. Chem. Soc.* **2013**, *135*, 14110−14118. (d) Schiwon, R.; Klingan, K.; Dau, H.; Limberg, C. *Chem. Commun.* **2014**, *50*, 100−102. (e) Stracke, J. J.; Finke, R. G. *ACS Catal.* **2014**, *4*, 909−933. (f) Stracke, J. J.; Finke, R. G. *ACS Catal.* **2014**, *4*, 79−89.

(10) (a) Wang, H.-Y.; Mijangos, E.; Ott, S.; Thapper, A. *Angew. Chem., Int. Ed.* **2014**, *53*, 14499−14502. (b) Song, F.; Ding, Y.; Ma, B.; Wang, C.; Wang, Q.; Du, X.; Fu, S.; Song, J. *Energy Environ. Sci.* **2013**, *6*, 1170−1184. (c) Lv, H.; Song, J.; Geletii, Y. V.; Vickers, J. W.;




DOI: 10.1021/acscatal.5b01101
*ACS Catal.* 2015, 5, 4994−4999

Sumliner, J. M.; Musaev, D. G.; Kögerler, P.; Zhuk, P. F.; Bacsa, J.; Zhu, G.; Hill, C. L. *J. Am. Chem. Soc.* **2014**, *136*, 9268−9271.
(11) (a) Brunschwig, B. S.; Chou, M. H.; Creutz, C.; Ghosh, P.; Sutin, N. *J. Am. Chem. Soc.* **1983**, *105*, 4832−4833. (b) Shafirovich, V. Y.; Khannanov, N. K.; Strelets, V. V. *Nouv. J. Chim.* **1980**, *4*, 81−84. (c) Harriman, A.; Porter, G.; Walters, P. *J. Chem. Soc., Faraday Trans. 2* **1981**, *77*, 2373−2383.
(12) (a) Zidki, T.; Zhang, L.; Shafirovich, V.; Lymar, S. V. *J. Am. Chem. Soc.* **2012**, *134*, 14275−14278. (b) Ullman, A. M.; Liu, Y.; Huynh, M.; Bediako, D. K.; Wang, H.; Anderson, B. L.; Powers, D. C.; Breen, J. J.; Abruna, H. D.; Nocera, D. G. *J. Am. Chem. Soc.* **2014**, *136*, 17681−17688.
(13) Gerken, J. B.; McAlpin, J. G.; Chen, J. Y. C.; Rigsby, M. L.; Casey, W. H.; Britt, R. D.; Stahl, S. S. *J. Am. Chem. Soc.* **2011**, *133*, 14431−14442.
(14) Minguzzi, A.; Fan, F.-R. F.; Vertova, A.; Rondinini, S.; Bard, A. J. *Chem. Sci.* **2012**, *3*, 217−229.
(15) Wang, H.-Y.; Mijangos, E.; Ott, S.; Thapper, A. *Angew. Chem., Int. Ed.* **2014**, *53*, 14499−14502.
(16) Schaffer, S. C.; Schaffer, C. E. *J. Chem. Educ.* **1996**, *73*, 180−181.
(17) (a) Chen, Z.; Concepcion, J. J.; Hu, X.; Yang, W.; Hoertz, P. G.; Meyer, T. J. *Proc. Natl. Acad. Sci. U. S. A.* **2010**, *107*, 7225−7229. (b) Klingan, K.; Ringleb, F.; Zaharieva, I.; Heidkamp, J.; Chernev, P.; Gonzalez-Flores, D.; Risch, M.; Fischer, A.; Dau, H. *ChemSusChem* **2014**, *7*, 1301−1310.
(18) Strmcnik, D.; Kodama, K.; van der Vliet, D.; Greeley, J.; Stamenkovic, V. R.; Markovic, N. M. *Nat. Chem.* **2009**, *1*, 466−472.
(19) Mech, K.; Zabinski, P.; Kowalik, R. *J. Electrochem. Soc.* **2013**, *160*, D246−D250.
(20) Du, J.; Chen, Z.; Chen, C.; Meyer, T. J. *J. Am. Chem. Soc.* **2015**, *137*, 3193−3196.



DOI: 10.1021/acscatal.5b01101
*ACS Catal.* 2015, 5, 4994−4999